

The 3' Untranslated Region of Sindbis Virus Represses Deadenylation of Viral Transcripts in Mosquito and Mammalian Cells[∇]

Nicole L. Garneau,[†] Kevin J. Sokoloski,[†] Mateusz Opyrchal, C. Preston Neff,
Carol J. Wilusz, and Jeffrey Wilusz*

Colorado State University, Department of Microbiology, Immunology and Pathology, Fort Collins, Colorado

Received 1 June 2007/Accepted 23 October 2007

The positive-sense transcripts of Sindbis virus (SINV) resemble cellular mRNAs in that they possess a 5' cap and a 3' poly(A) tail. It is likely, therefore, that SINV RNAs must successfully overcome the cytoplasmic mRNA decay machinery of the cell in order to establish an efficient, productive infection. In this study, we have taken advantage of a temperature-sensitive polymerase to shut off viral transcription, and we demonstrate that SINV RNAs are subject to decay during a viral infection in both C6/36 (*Aedes albopictus*) and baby hamster kidney cells. Interestingly, in contrast to most cellular mRNAs, the decay of SINV RNAs was not initiated by poly(A) tail shortening in either cell line except when most of the 3' untranslated region (UTR) was deleted from the virus. This block in deadenylation of viral transcripts was recapitulated in vitro using C6/36 mosquito cell cytoplasmic extracts. Two distinct regions of the 319-base SINV 3' UTR, the repeat sequence elements and a U-rich domain, were shown to be responsible for mediating the repression of deadenylation of viral mRNAs. Through competition studies performed in parallel with UV cross-linking and functional assays, mosquito cell factors—including a 38-kDa protein—were implicated in the repression of deadenylation mediated by the SINV 3' UTR. This same 38-kDa protein was also implicated in mediating the repression of deadenylation by the 3' UTR of another alphavirus, Venezuelan equine encephalitis virus. In summary, these data provide clear evidence that SINV transcripts do indeed interface with the cellular mRNA decay machinery during an infection and that the virus has evolved a way to avoid the major deadenylation-dependent pathway of mRNA decay.

The *Alphavirus* genus of the *Togaviridae* family consists primarily of a group of viruses with single-stranded, positive-sense RNA genomes that are transmitted by arthropods and replicate exclusively within the cytoplasm of infected cells (45, 51). Sindbis virus (SINV), the prototypic virus of the genus, encodes genomic and subgenomic RNAs that are capped on the 5' terminus, polyadenylated at the 3' end, and contain 5' and 3' untranslated regions (UTRs) similar to cellular mRNAs. The viral genomic RNA, in fact, functions as an mRNA immediately upon infection. This strategy of mimicking cellular mRNAs has potential advantages and disadvantages for the virus. While this strategy allows viral RNAs to be effectively translated, viral transcripts may also be fully subject to the activity of the mRNA decay machinery within the cytoplasm of the host cell. Aspects of this anticipated interplay between SINV transcripts and cellular mRNA decay enzymes were investigated in this study.

The regulation of mRNA decay plays a major role in gene expression within eukaryotic cells. In some cases, more than 50% of the changes in gene expression when cells are stimulated or forced to adapt to nutrient changes are, in fact, due to this posttranscriptional regulatory process (6, 7, 21, 32). Furthermore, the RNA turnover machinery also plays a very active

role in the quality control of gene expression through processes like nonsense-mediated mRNA decay (5). The predominant mRNA decay pathway in eukaryotes initiates with shortening of the poly(A) tail. This deadenylation process is considered to be a major, rate-limiting step of mRNA turnover (8, 10, 11, 55, 60). Numerous deadenylase enzymes have been identified, the major characterized ones being the CCR4/CAF1 complex, PAN2/3, and poly(A) RNase (PARN) (31, 47, 54, 60). Following shortening of the poly(A) tail, the deadenylated mRNA is then subject to one of two exonucleolytic processes resulting in the highly processive degradation of the transcript (13, 22). In one pathway, the 5' cap structure can be removed via the decapping proteins DCP1/DCP2, leaving the mRNA open to attack by the 5'-to-3' exoribonuclease XRN1 (48). Alternatively, removal of the poly(A) tail makes the mRNA vulnerable to 3'-5' exonucleolytic decay by a large complex of proteins called the exosome (27). Alternative pathways also exist in which mRNA decay can occur by deadenylation-independent decay or endonucleolytic cleavage, including the targeting of transcripts for decay by small interfering RNAs and microRNAs (14, 41, 44).

We have previously described an in vitro assay using cytoplasmic extracts from HeLa cells that faithfully reproduces many aspects of regulated mRNA decay (19). Recently, we have extended this in vitro technology to cytoplasmic extracts from *Aedes albopictus* C6/36 cells with similar success (42, 49). Establishment of an in vitro mRNA decay system in cytoplasmic extracts from mosquito cells, a vector host of many viruses, including alphaviruses such as SINV, affords us a valuable assay to address mechanistic questions regarding

* Corresponding author. Mailing address: Colorado State University, Department of Microbiology, Immunology and Pathology, 1682 Campus Delivery, Fort Collins, CO 80523-1682. Phone: (970) 491-0652. Fax: (970) 491-4941. E-mail: jeffrey.wilusz@colostate.edu.

[†] N.L.G. and K.J.S. contributed equally to this work.

[∇] Published ahead of print on 31 October 2007.

the interaction between SINV RNAs and key mRNA decay enzymes.

Since alphavirus RNAs resemble cellular mRNAs in that they have a cap and a poly(A) tail, upon infection SINV transcripts should be confronted by this very efficient cellular mRNA decay machinery within the cytoplasm. It is very likely that SINV and other RNA viruses have adapted ways to protect their polyadenylated transcripts from rapid degradation by these enzymes and pathways. Such protective features may include the presence of mRNA stabilizer elements (10), strong RNA structures (18, 40), and perhaps novel messenger ribonucleoprotein constituents (25). To date, relatively little is known about the interactions between RNA viruses and the cellular mRNA turnover machinery; we wished to investigate the potential influence of this process on SINV RNAs in host cells.

In this study we first took advantage of a temperature-sensitive mutation in the viral RNA polymerase to establish an approach which would allow us to selectively measure the rate of decay of SINV RNAs in mosquito and baby hamster kidney (BHK) cells. Interestingly, SINV RNAs have evolved a method to block deadenylation of their RNAs via sequence elements in the 3' UTR, allowing them to circumvent the major pathway of cellular mRNA decay as well as maintain the polyadenylated status of their transcripts for efficient translation. This block in deadenylation was reproduced *in vitro* using cytoplasmic extracts from mosquito cells, and this system was exploited to gain mechanistic insights into the repression of deadenylation by SINV. A combination of elements located in the viral 3' UTR was found to contribute to the repression of deadenylation, including the conserved pattern of repeat sequence elements (RSEs) which to date have no known function. Interestingly, the 3' UTR from Venezuelan equine encephalitis virus (VEEV) also blocked poly(A) shortening *in vitro*. Finally, evidence for a *trans*-acting cellular factor that contributes to the repression of deadenylation was obtained. Collectively, these data represent clear evidence that SINV RNAs have adapted ways to thwart a major and often rate-limiting aspect of the mRNA decay machinery.

MATERIALS AND METHODS

Cell lines. BHK-21 cells and African green monkey cells (Vero) were grown at 37°C in 5% CO₂ in HyQ minimal essential medium-Earle's balanced salt solution (HyClone) supplemented with 10% heat-inactivated fetal bovine serum, nonessential amino acids, L-glutamine, and penicillin/streptomycin. Adherent *A. albopictus* (C6/36) cells were obtained from the ATCC and grown in the same medium described above at 28°C in 5% CO₂ and were used for all experiments involving viral infections. C6/36 suspension cells were obtained from Jon Carlson and Erica Suchman (Colorado State University) and grown in SF900 II medium (Gibco) supplemented with penicillin/streptomycin in spinner flasks at room temperature (52). These suspension cells were used to make extracts for use in our cell-free deadenylation assays.

Cell extracts. C6/36 cytoplasmic S100 extracts were prepared as described previously (42, 49) with several modifications. Briefly, cells were collected by centrifugation and washed in ice-cold phosphate-buffered saline. The washed cells were suspended in three packed cell volumes of buffer A (10 mM HEPES, pH 7.9, 1.5 mM MgCl₂, 10 mM KCl, 1 mM dithiothreitol [DTT]) and allowed to swell on ice for 10 min. Following a brief centrifugation, the swollen cells were resuspended in 1 volume of buffer A and lysed by Dounce homogenization. The lysate was centrifuged at 2,000 × *g* to remove nuclei, and the supernatant was transferred to a fresh tube. The salt concentration was adjusted by the addition of 0.11 volumes of buffer B (300 mM HEPES, pH 7.9, 30 mM MgCl₂, 1.4 mM KCl, 1 mM DTT), and the lysate was centrifuged at 100,000 × *g* for 1 h. Glycerol

was added to the supernatant to a final concentration of 20%, and aliquots were stored at -80°C. The S100 extracts are stable at this temperature for several months.

Virus stocks. An AR339 SINV cDNA clone (pToto1101/ts6) (4) was kindly provided by Margaret Macdonald (Rockefeller University, NY). The viral cDNA clone was linearized with XhoI and used as a template for *in vitro* transcription. A SINV clone containing all of its 3' UTR deleted except for the conserved sequence element (CSE) region was generated as follows: pToto1101/ts6 was cut with NdeI and XhoI, and the resulting fragment was subcloned into pGem4. PCR with the primers SV Δ Jump L (5'-AGGCGTACGTGCAATTGTCCAGCAGATT-3') and SV Δ Jump R (5'-CCCTCGAGGAATCCCTTGGAAATGTTAAAAACAAAATTCATCTTCGTGTGCTAGTCAGC-3') was used to jump from the CSE of the 3' UTR directly to the 3' end of the structural open reading frame, excluding the 3' UTR, leaving the insert flanked with a BsiWI at the 5' end and XhoI at the 3' end. The original pToto1101 was cut with BsiWI and XhoI to excise the wild-type sequence containing the 3' UTR, and this sequence was replaced by ligation of the gel-purified PCR product. The resulting pToto1101/ts/6/Δ3' UTR plasmid was linearized and transcribed as described above for pToto1106/ts6.

SINV stocks were produced by electroporation of transcription products into BHK-21 cells using a BTX EMC 630 apparatus (2 pulses at 400 LV, 800Ω, and 25 μF). Virus present in the medium 24 to 48 h later was harvested and amplified by one passage on BHK-21 cells. Amplified virus was collected 24 to 48 h postinfection, and plaque assays were performed on Vero cells to determine titers.

Preparation of RNA substrates, RNA probes, and competitor RNAs. Internally labeled substrate and probe RNAs were prepared by *in vitro* transcription from linearized plasmid DNA templates and gel purified as previously described (57). Unlabeled competitor RNAs were generated using a MEGAscript High Yield Transcription kit (Ambion) according to the manufacturer's recommendations.

The deadenylation marker for the polylinker-derived reporter RNA was transcribed using SP6 from the pGem-4 plasmid (Promega) linearized with HindIII. To generate a matched reporter RNA containing a PAT, we inserted a 60-base adenylate (A60) stretch followed immediately by an NsiI restriction site downstream of the HindIII site of pGem-4 to create the plasmid pGem-A60. Cleavage of the plasmid with NsiI and transcription using SP6 RNA polymerase generates a reporter RNA that contains a 60-base adenylate tract precisely at its 3' end.

A template for generating the SINV-3' UTR-A60 RNA was obtained by inserting a 319-nucleotide (nt) fragment representing the SINV 3' UTR between the EcoRI and PstI sites of pGem-A60. This placed the insert within 12 bases of the PAT. The insert was generated by PCR from a DNA clone containing the entire MRE16 SINV genome (accession number U90536) obtained from Carol Blair (Colorado State University) using the primers 5' CGGAATTTCCGCTACGCCAAATGACCCG and 5' GAAATATTAATAAACAATAATTCAGCTGTT. Cleavage of the plasmid with NsiI generated a template to create SINV-3' UTR-A60 RNA that contained a PAT. The SINV 3' UTR was divided into three segments using a PCR or direct oligonucleotide cloning approach and cloned into the EcoRI and PstI sites of the pGem-A60 vector. pSINV-RSE contains the region from the start of the 3' UTR through 60 bases from the 3' end. pSINV-URE contains the U-rich region represented by the oligonucleotides 5'-AATTCTCATAATCAATGTATTATTGTCTTGTATTGTATTTCACATATGCA and 5'-GTATGTGAATACAATAACAAGACAATAATACATTGATTATGAG. pSINV-CSE contains the 3' terminal 19 bases of the SINV 3' UTR.

To generate a plasmid expressing a polyadenylated version of the 3' UTR of VEEV, the 3' noncoding region was isolated by PCR using the primers 5'-GGCGAATTTGAATCAGCAGCAATTGGC and 5'-GGCCTGCAGGAAATTAATAAACAATAATCC (in collaboration with Richard Kinney of the CDC). The PCR product was inserted into the EcoRI-PstI sites of pGEM-A60 vector. Transcription using SP6 of NsiI-linearized templates yielded VEEV 3' UTR-A60 RNA.

A number of studies were performed using an isolated SINV RSE along with a series of mutant derivatives. Templates to generate the SINV-RSE3 sequence were obtained by annealing two DNA oligomers, 5' AAAACTCAATGTATTCTGAGGAAGCGTGGTGCAGAAATGCCACGC and 5'-GCGTGGCATTATGCACCACGCTTCCCTCAGAAATACATTGAGTTTT, and inserting the fragment into the EcoRI-PstI sites of pGemA60. The four RSE3 mutants were constructed in a similar fashion using the following oligonucleotides (mutated bases are underlined): m5,7, 5' AAAAGTGAATGTATTTCTGAGGAAGCGTGGTGCAGAAATGCCACGC and 5'-GCGTGGCATTATGCACCACGCTTCTCAGAAATACATTCACTTTT; m9-16, 5' AAAACTCATACATAAACTGAGGAAGCGTGGTGCAGAAATGCCACGC and 5'-GCGTGGCATTATGCA CCACGCTTCCCTCAGTTTTATGTATGAGTTTT; m19,21, 5' AAAACTCAATGTATTTCTCACGAAGCGTGGTGCAGAAATGCCACGC and 5'-GCGTGG

CATTATGCACCACGCTTCGTGAGAATACATTGAGTTTT; and m32-38, 5'-AAAACCTAATGTATTCTGAGGAAGCGTGGTCTGATTAGCCACGC and 5'-GCGTGGCTAATACGACCACGCTTCCTCAGAAATACATTGAGT TTT.

To generate a probe to detect SINV RNAs in RNase protection assays, the primers 5'-ATAGGATCCCCGTGACGACCCGGTATGAGGTAGA and 5'-C ATAAGCTTTTTGAGAAGCCAGCCCGTTGCG were used to amplify a DNA fragment that spanned the genomic/subgenomic junction of SINV (bases 7471 to 7760 [accession number NC001547]). The probe was designed to overlap the junction so that it would be capable of discerning both genomic and subgenomic RNAs based on the size of the fragment protected from RNase digestion. PCR products were cloned into the BamHI-Hind III sites of pGem-4. Plasmids were linearized with BsrGI and transcribed using T7 RNA polymerase. To generate a probe for detecting the ribosomal protein S5 (RPS5) mRNA in RNase protection assays (RPAs), the primers 5'-ATTACATCGCCGTCAGGAG and 5'-TCTTGATGGCGTACGAGTTG were used to amplify cDNA obtained from C6/36 cells and inserted into the pGemT-easy vector. Plasmid DNA was cut with NcoI and transcribed using SP6 RNA polymerase to generate an RPS5-specific probe. To generate a probe for detecting the 5S rRNA in RPAs, the primers 5'-TCTCGTCTGATCTCGGAAGC and 5'-AACCAGCCA AAAAGCCTACA were used to amplify cDNA obtained from BHK-21 cells and inserted into the pGemT-easy vector. Plasmid DNA was cut with NcoI and transcribed using SP6 RNA polymerase to generate a 5S RNA-specific probe.

Probes to detect transcripts from the wild-type SINV *ts6* strain in RNase/Northern experiments were derived from the 3' UTR of SINV by PCR amplification of an infectious DNA clone of TR339 (kindly provided by Ken Olson, Colorado State University) using the primers 5'-CCGAATTCCTGACGCCCCAATGATCC and 5'-AAACTGCAGGAAATGTTAAAAACAATTT. Reaction products were cloned into pGem-4. Linearization of this plasmid with EcoRI and transcription by T7 RNA polymerase generated a probe complementary to the 3' UTR of the virus. Probes to detect transcripts generated by the $\Delta 3'$ UTR SINV were constructed by inserting a Sall-EcoRI fragment from the pToto1101/*ts6*/ $\Delta 3'$ UTR clone described above into pGem-4. Linearization with HindIII and transcription using SP6 RNA polymerase generated the desired riboprobe.

In vivo viral RNA decay assay. To measure the *in vivo* half-lives of SINV RNAs, confluent C6/36 mosquito adherent cell monolayers or BHK cells were infected at a multiplicity of infection of 5 in complete growth medium. Following 1 h of incubation at 28°C, the inoculum was removed, fresh complete medium was added, and the cells were incubated at 28°C for 10 h. The cells were then shifted to the nonpermissive temperature (40°C), and total RNA was extracted using the Trizol method (Invitrogen) at various time points following the shift. The quantity and identity of viral RNA in each time point were assayed by an RPA using the SINV subgenomic junction RNA probe described above. RPS5 mRNA (for C6/36 cells) and 5S rRNA (for BHK cells) were routinely detected using the riboprobes described above as loading controls to ensure the validity of all quantitation. The protected RNAs were resolved on a 5% polyacrylamide gel containing 7 M urea and visualized using a Bio-Rad Molecular Imager FX. RNA quantification was determined using Bio-Rad Quantity One software. The half-lives shown are averages of two separate viral preparations and six independent assays.

Analysis of *in vivo* poly(A) tail lengths. For RNase H/Northern assays, total RNA samples from infected-cell time courses described above were hybridized to a DNA oligonucleotide (5'-TAGTGTGCTATATTGCCCGC) designed to anneal to the region of the SINV 3' UTR between RSE1 and RSE2 and treated with RNase H. This step was performed to reduce the size of SINV RNAs that would be detected by Northern blotting so that the length of the poly(A) tail could be readily discerned on a polyacrylamide gel. Additional reactions also included oligo(dT) to generate a marker for fully deadenylated viral RNAs. The size of the poly(A) tail of the mRNA could then be determined by comparison of the bands detected to the position of this fully deadenylated marker. Reaction products were separated on a 5% denaturing polyacrylamide gel, electroblotted to a Hybond-XL (GE Healthcare) membrane, and probed with the SINV-specific probes outlined above. Following several washes, results were analyzed by phosphorimaging (62).

Linker ligation-mediated poly(A) tail (LLM-PAT) assays assess poly(A) tail length via the ligation of a linker to the 3' end of all mRNAs, followed by PCR amplification using a virus-specific upstream primer. RNA collected during the half-life time course described above (following temperature shift) was ligated to 5' pppRNA linker (5'-rApppTTTAACCGCAATTCCAG/3ddC, where r is ribonucleotide; Integrated DNA Technologies Linker 3) at 16°C for 2 h in 50 mM Tris-Cl, pH 7.5, 10 mM MgCl₂, 20 mM DTT, and 0.1 mg/ml bovine serum albumin. The ligated RNA was then reverse transcribed using a PAT reverse

transcription primer specific to the RNA linker (5'-CTGGAATTCGCGGT). The resulting cDNA was then amplified by PCR using the PAT(dT) reverse transcription-PCR primer (5'-CTGGAATTCGCGGTTAAATTT) and a primer specific to the virus used: LLM-PAT *ts6*100bp, 5'-GGACGCCAAA AACTCAATGT; LLM-PAT *ts6*/ $\Delta 3'$ UTRmut100bp, 5'-GTTGGCTGTTTGC CCTTTTC. PCR products were separated on a 5% nondenaturing gel. Following electrophoresis, the gel was soaked in 1× Tris-borate-EDTA buffer with Sybr Green I nucleic acid gel stain (Invitrogen) and visualized using a Typhoon Trio imager.

In vitro mRNA deadenylation assays. Deadenylation assays using C6/36 extracts were performed as described previously (42) with minor modifications. Briefly, a typical 27- μ l reaction mixture contained 100,000 cpm (5 to 40 fmoles) of internally labeled RNA, 2.4% polyvinyl alcohol, 17.5 mM phosphocreatine, 0.7 mM ATP, 25 ng/ μ l poly(A) (Sigma), 20 units of RNase inhibitor, and 60% (vol/vol) C6/36 S100 cytoplasmic extract. Poly(A) RNA is added to these reactions to sequester poly(A) binding proteins and allow for efficient deadenylation to occur (42). For competition experiments, reaction mixtures also contained the amounts of competitor RNA indicated in the figures. Reaction mixtures were incubated at 28°C for the indicated times. Reaction products were recovered by phenol-chloroform extraction and ethanol precipitation, separated on a 5% polyacrylamide gel containing 7 M urea, and visualized using a Bio-Rad Molecular Imager FX. Results were quantified by assessing the relative level of fully deadenylated RNA versus the total RNA in the sample using Quantity One software. All experiments were repeated at least three times with similar results.

UV cross-linking assays. UV cross-linking assays were performed as previously described (57) with some minor modifications. Cross-linking assays using C6/36 extracts were prepared as described above for deadenylation assays with the addition of 5 mM EDTA to block RNA decay and allow for accurate comparison between samples. Following a brief incubation at room temperature, proteins were cross-linked to the radiolabeled RNA substrates by 254-nm UV light (180 mJ) using a UV Stratalinker 2400 (Stratagene). Samples were treated with RNase A/RNase One (which cleaves 3' to all RNA bases) for 15 min at 37°C, and proteins cross-linked to short radioactive RNA oligomers were separated on 10% polyacrylamide gels containing sodium dodecyl sulfate (SDS) and visualized by phosphorimaging.

RESULTS

SINV RNAs have measurable decay rates. A quantitative assessment of the half-lives of SINV RNAs within an infected cell has not been performed to date. The best way to assess the relative stability of a specific transcript is to selectively target and inhibit its synthesis, thereby minimizing off-target effects (59). Therefore, to determine if SINV RNAs are degraded by the host-cell mRNA decay machinery during infection, we developed an *in vivo* assay using the SINV *ts6* strain that contains a temperature-sensitive mutation in the RNA-dependent RNA polymerase (4). Viral RNA synthesis is effectively shut off in the SINV *ts6* strain when cells are shifted to 40°C (4). C6/36 mosquito cells were infected with this temperature-sensitive virus, and replication was allowed to progress for 10 h to select for a time during acute infection when viral subgenomic RNA synthesis is robust (30, 33). After 10 h, cells were shifted to the nonpermissive temperature (40°C) to selectively turn off viral transcription, and RNA was isolated over a time course and analyzed using an RPA. As seen in Fig. 1A and B, although viral genomic and subgenomic transcripts had vastly different decay rates, both were measurable. The genomic RNA was very stable, with a half-life of greater than 10 h. This observation was expected as a significant percentage of genomic RNA is likely to be packaged (51) and therefore resistant to decay. However, the subgenomic RNA of SINV, which is free in the cytoplasm while interacting with cytoplasmic translation (and perhaps other) machineries, was only moderately stable, with a half-life of 3.9 ± 0.6 h. Similar data were obtained for independent virus preparations and infec-

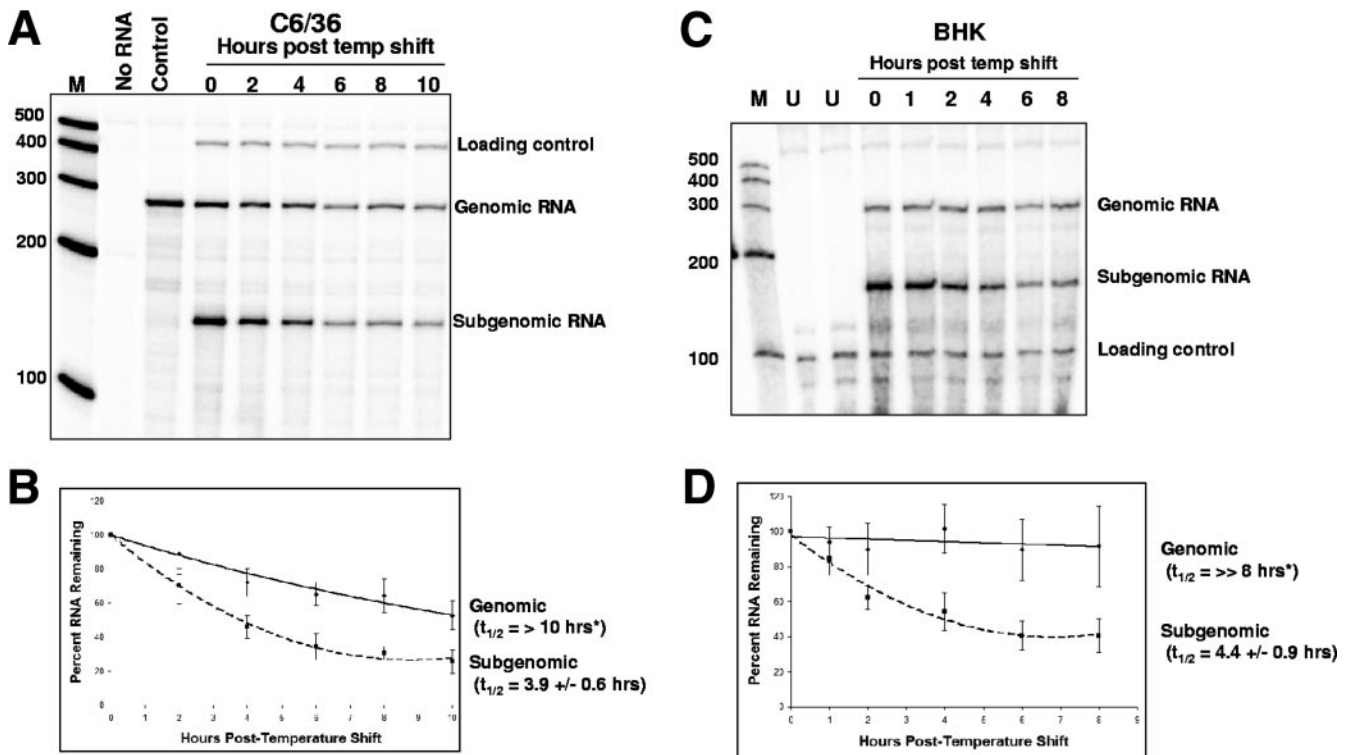


FIG. 1. SINV RNAs exhibit measurable half-lives in C6/36 cells. (A) C6/36 mosquito cells were infected with a SINV variant containing a temperature-sensitive mutation in its RNA polymerase gene. At 10 h postinfection, cells were shifted to 40°C (temp shift) to shut off viral transcription, and total RNA samples were taken at the indicated times and probed for viral specific transcripts by RPA. The level of the mRNA for RPS5 was detected concurrently to allow normalization of all samples for accurate quantitation. Reaction products were separated on a 5% polyacrylamide gel containing 7 M urea and visualized by phosphorimaging. The lane labeled No RNA represents the results obtained when no total cellular RNA was added to the reaction mixture, and the lane indicated control represents an RPA performed on in vitro transcribed SINV genomic RNA. (B) Graphical representation of the data obtained from six independent replicates of RPAs performed as shown in panel A. (C) BHK cells were infected with the SINV *ts6* variant, and samples were treated as outlined above for panel A. (D) Graphical representation of the data shown in panel C. As in panel B, each data point represents the average of two independent virus preparations and six assays. The data points were plotted in Excel with a second-order polynomial trend line to reflect the potential biphasic decay. $t_{1/2}$, half-life.

tions, and in all experiments, mRNA for the RPS5 was probed for as a loading control to ensure accurate quantitation. While not as stable as a mosquito mRNA for a housekeeping gene (e.g., RPL31), SINV subgenomic RNA was more stable than the average class of *A. albopictus* mRNAs (La, STAT, and AchE) with intermediate half-lives of 2.5 to 4.5 h, and vastly more stable than the cellular mRNAs Usp, Ecr1, and IAP1 (half-lives of ≤ 1 h) which we previously reported using C6/36 cells (42). As seen in Fig. 1C and D, similar data were obtained for the stability of viral transcripts when infections were performed in BHK cells, suggesting that our initial observations made in insect cells could be generalized to mammalian cells. Finally, it should be noted that the graphs in Fig. 1B and D were plotted with a second-order polynomial trend line. Although we attempted to fit the data to a linear curve, the correlation coefficients associated with the polynomial trend line better represented the data. These data therefore suggest potential biphasic decay kinetics for viral transcripts. This may be reflective of the innate mechanism of viral mRNA decay inside cells, multiple populations of viral RNAs, and/or changes in the cellular mRNA decay machinery over time as a consequence of viral infection or temperature shift.

In summary, we conclude that SINV RNAs are in fact rec-

ognized by the mRNA decay machinery during infection. Furthermore, these data suggest that SINV transcripts, although susceptible to mRNA decay, appear to have evolved a means of slowing the process, directing us to look more closely at the mechanism involved.

SINV RNAs decay in a deadenylation-independent manner. In every eukaryotic organism where mRNA decay has been assessed (including insects), cellular mRNAs decay in a predominantly deadenylation-dependent fashion (22, 42). Furthermore, the deadenylation step appears to be rate-limiting in the decay of most cellular mRNAs (60). For this reason, we first wanted to determine if SINV RNAs were substrates for the major cellular mRNA degradation pathway and were therefore deadenylated prior to decay. In order to detect changes in the length of the viral poly(A) tail during mRNA decay, total RNA samples collected from the in vivo approach described in the legend of Fig. 1 were hybridized to a SINV 3' UTR-specific DNA oligonucleotide and treated with RNase H to cleave SINV transcripts into two pieces. This treatment reduced the size of the viral transcript that would be detected by Northern blotting to ~ 200 nt in order to improve resolution of poly(A) tail size. Using similar analyses, it is well established that cellular mRNAs undergo deadenylation prior to decay (8,

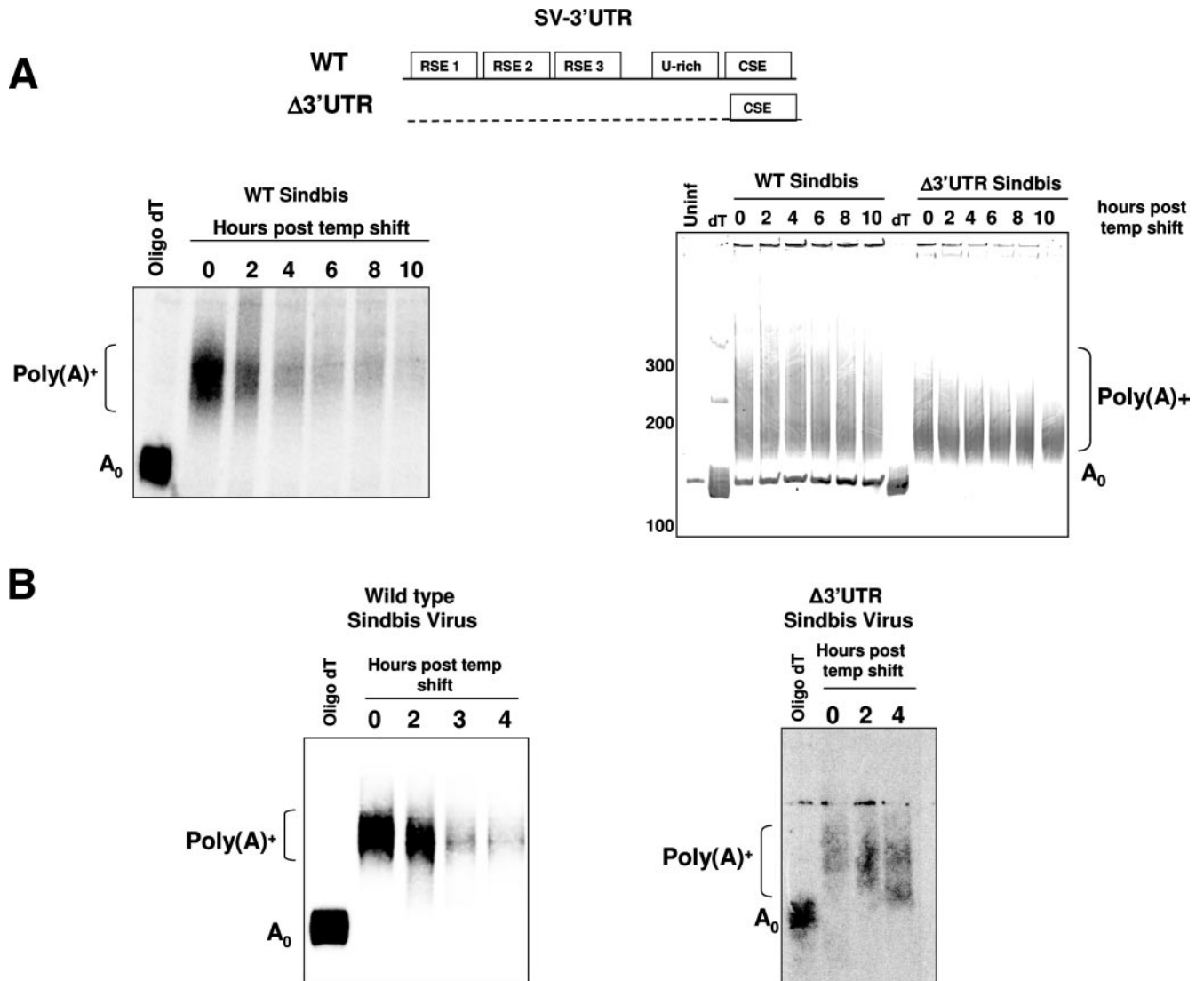


FIG. 2. SINV RNAs decay in a deadenylation-independent fashion due to the presence of the 3' UTR. (A) Diagrammatic representation of the 3' UTR of the wild-type (WT) and Δ 3' UTR viruses (SV) used in these studies (top). C6/36 mosquito cells were infected with an SINV variant containing a temperature-sensitive mutation in its RNA polymerase gene and an intact 3' UTR (left panel). At 10 h postinfection, cells were shifted to 40°C to shut off viral transcription, and total RNA samples were isolated at the indicated times. RNAs were hybridized to a DNA oligonucleotide designed to bind to the region of the SINV 3' UTR and treated with RNase H. Samples for the lane marked Oligo(dT) were also hybridized to oligo(dT) prior to RNase H treatment to generate a marker for fully deadenylated viral mRNAs. Reaction products were separated on a 5% polyacrylamide gel, electroblotted to Hybond-XL membranes, and probed with SINV-specific probes. Results were visualized by phosphorimaging. The PAT length of viral-specific transcripts in RNA samples from C6/36 infections by a SINV *ts6* strain containing either a wild-type 3' UTR (left) or with a deleted 3' UTR as outlined in the diagram (Δ 3' UTR Sindbis) prepared as described above was determined by a PCR-based LLM-PAT approach, and products were analyzed by agarose gel electrophoresis (right panel). RNAs were hybridized to oligo(dT) (lanes dT) and digested with RNase H prior to LLM-PAT analysis. The Uninf lane shows the products of an LLM-PAT assay done on total RNA from uninfected C6/36 cells using the primer set to detect SINV transcripts with a wild-type 3' UTR. The position of molecular size markers is shown on the left. (B) BHK cells were infected with either the SINV *ts6* strain (left) or a variant (right) that contains a substantial deletion in its 3' UTR outlined in the top panel. The RNase H cleavage/Northern blot procedure outlined in the legend of panel A was used to visualize the PAT of viral transcripts. The positions of fully deadenylated (A_0) and poly(A)⁺ RNAs are indicated to the left of each panel. WT, wild type; temp, temperature.

23, 29, 34, 38, 43, 55, 58, 60). Surprisingly, the poly(A) tail of SINV transcripts did not appreciably shorten as the viral RNA was degraded over the time course in either C6/36 mosquito cells (Fig. 2A, left panel) or BHK cells (Fig. 2B, wild-type virus). In order to directly assess whether the 3' UTR played a role in repressing deadenylation in tissue culture cells, we constructed a SINV mutant virus in which the entire 3' UTR

except for the CSE was deleted (outlined in Fig. 2A). As seen in the right panels of Fig. 2A and B, this deletion in the 3' UTR of SINV allowed deadenylation of viral transcripts in both BHK and C6/36 cells. We analyzed poly(A) length by a sensitive, yet more qualitative PCR-based LLM-PAT assay for infections with the Δ 3' UTR SINV mutant in C6/36 cells due to the fact that this viral mutant grows very poorly in mosquito

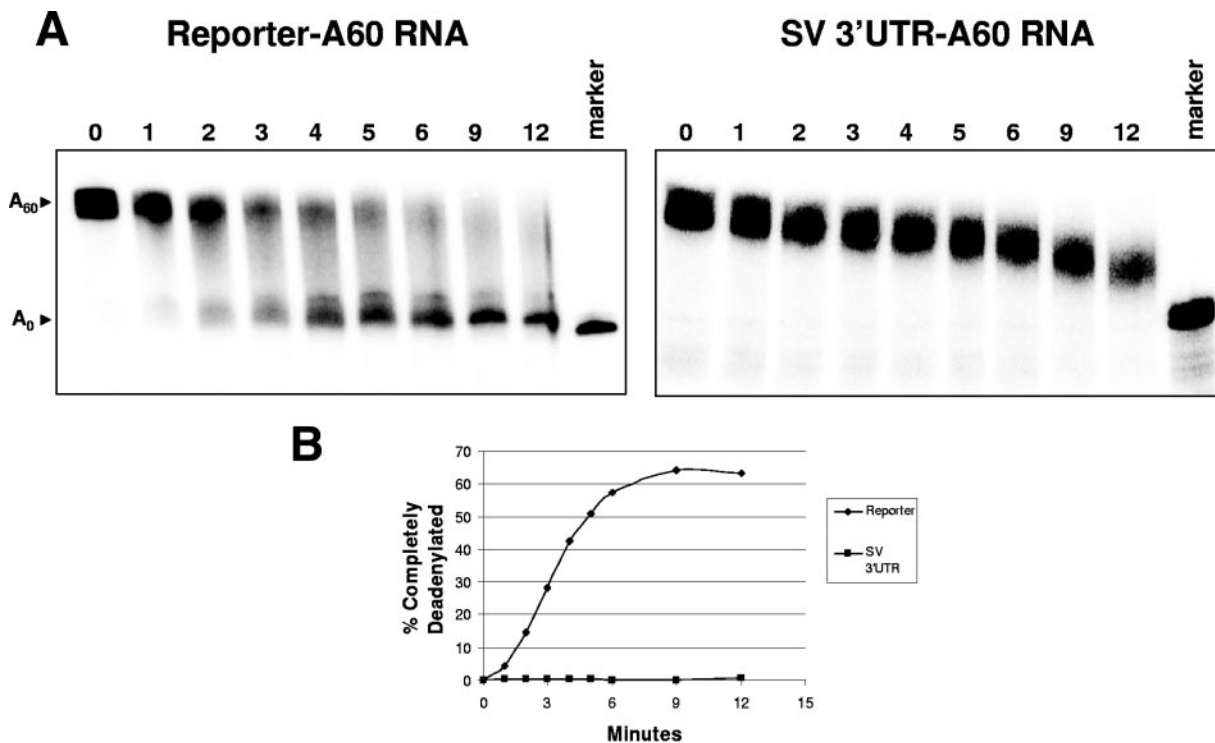


FIG. 3. The 3' UTR of SINV represses deadenylation in C6/36 cytoplasmic extracts. (A) A polyadenylated reporter RNA (A_{60}) derived from the polylinker region (EcoRI to HindIII) of pGem-4 (left) or a variant containing the 3' UTR of SINV (SV) (right) was incubated in an in vitro RNA deadenylation/decay system derived from C6/36 S100 cytoplasmic extracts for the indicated times. Reaction products were analyzed on a 5% polyacrylamide gel containing 7 M urea and visualized by phosphorimaging. The marker lane denotes fully deadenylated versions of the input transcript. (B) Graphical representation of the data shown in panel A. Similar data were obtained from multiple independent replicates.

cells (33; also data not shown). In the data derived from the LLM-PAT assay, note that a nonspecific band of around 140 bases is detected in RNA samples from both infected and uninfected cells using the probe set to detect viral RNAs with a wild-type 3' UTR. Also note that due to significant differences in the magnitude of replication of $\Delta 3'$ UTR mutant virus relative to wild type, we have encountered difficulties in detecting viral transcripts from $\Delta 3'$ UTR infections in a quantitative fashion. Therefore, we have only analyzed the mutant accurately for qualitative changes in poly(A) tail length. The apparent higher stability of $\Delta 3'$ UTR transcripts that one might infer from Fig. 2 is due to loading differences rather than true quantitative distinctions. These data highlight the dramatic effect that the $\Delta 3'$ UTR mutation is having on overall viral RNA expression. In summary, we conclude that the decay of SINV transcripts does not appear to occur via the predominant, deadenylation-dependent mRNA decay pathway in the cell and is likely proceeding via an alternative pathway. These observations suggest that SINV RNAs may possess a specific mechanism for inhibiting their deadenylation. In addition to influencing mRNA stability, maintenance of the poly(A) tail on viral mRNAs likely also ensures their efficient translation through the poly(A) binding protein-mediated recruitment of initiation factors.

The 3' UTR of SINV represses deadenylation in vitro. The majority of mRNA stability elements described to date are located within the 3' UTR (28). The SINV 3' UTR, specifically the 19-nt CSE at the extreme 3' end of the RNA, is absolutely

required for viral replication (24, 33, 35). Given the additional possible roles of the 3' UTR in translation and localization of SINV RNAs, any detailed in vivo analysis of the role of the 3' UTR during an infection would be difficult to interpret. Therefore, we chose to analyze the role of the SINV 3' UTR in mRNA decay using an in vitro assay which allows us to evaluate the effects of mutations on deadenylation without the involvement of other 3' UTR functions. We have previously reported an in vitro RNA deadenylation/decay assay using cytoplasmic extracts from C6/36 cells that reproduces many aspects of mRNA stability observed in vivo (42).

We inserted the SINV 3' UTR into a reporter RNA derived from the polylinker region of a derivative of the pGEM-4 plasmid that contained an encoded 60-base poly(A) tail so that the SINV 3' UTR was positioned proximal to the poly(A) tail. Reporter transcripts, with and without the SINV 3' UTR, were incubated with C6/36 cytoplasmic extracts in our in vitro RNA deadenylation system. As seen in Fig. 3, while the mosquito cell extracts rapidly deadenylated the reporter transcript, the RNA containing the SINV 3' UTR was deadenylated only very slowly. Although the Gem-4 polylinker-derived reporter RNA used in this experiment is significantly smaller than the SINV 3' UTR RNA, comparable rapid deadenylation kinetics were observed with control reporter RNAs derived from cellular mRNAs (data not shown). Consistent with reported observations of deadenylase activity, poly(A) shortening in these assays results in a short oligoadenylate tail on the RNA substrate (22). Whereas fully deadenylated products from the control

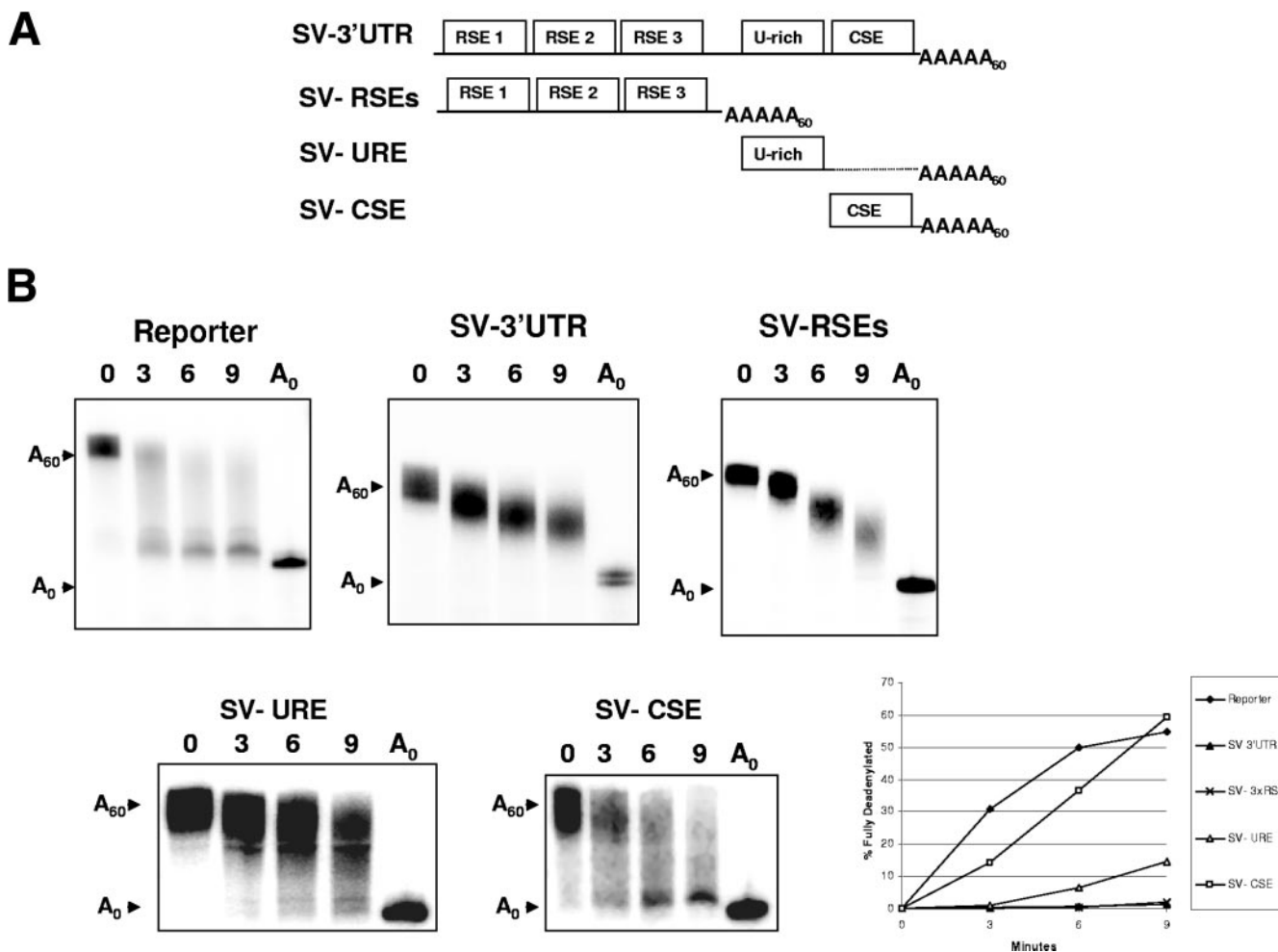


FIG. 4. A combination of 3' UTR elements contributes to efficiently repress deadenylation of SINV (SV) RNAs. (A) Graphical representation of the RNAs derived from the SINV 3' UTR RNAs used in this experiment. (B) A polyadenylated reporter RNA (Reporter) or variants containing the entire 3' UTR of SINV (SV-3' UTR), the 5' portion of the UTR that contains the RSEs (SV-RSEs), the U-rich region (SV-URE), or the CSE region (SV-CSE) were incubated in an *in vitro* RNA deadenylation/decay system derived from C6/36 S100 cytoplasmic extracts for the indicated times. Reaction products were analyzed on a 5% polyacrylamide gel containing 7 M urea and visualized by phosphorimaging. The lanes marked A_0 contain fully deadenylated versions of the input transcript. The graph at right represents the data shown in panel B. Similar data were obtained from multiple independent replicates.

reporter RNA were observed in as little as 2 min, the maximal amount of deadenylation that we observed on the SINV 3' UTR RNA was limited to 15 to 30 bases during the extent of the time course. From these data, we conclude that our *in vitro* system is capable of reproducing the repression of deadenylation that was observed in cells and that the 3' UTR sequence of the genomic and subgenomic RNAs was indeed responsible for the observed repression. Furthermore, these observations also provide us with a convenient and powerful assay to assess the specific effects of 3' UTR mutations specifically on the deadenylation process.

Multiple elements of the SINV 3' UTR contribute to the repression of deadenylation. As a first step toward dissecting the element(s) responsible for the repression of deadenylation that we observed with the SINV 3' UTR, we divided the region into several sections. The 5' segment (SINV-RSE) contained the three RSEs of SINV. RSEs are found in the 3' UTRs of all alphaviruses, but their function in viral biology is not yet un-

derstood (51). The 3' segment contained a U-rich region (SINV-URE) as well as the 19-nt conserved sequence element (SINV-CSE). The CSE is known to be absolutely required for efficient replication of the virus (33, 35). All SINV fragments were inserted between the EcoRI and PstI sites of the pGem4 reporter plasmid. These RNAs, which are outlined in Fig. 4A, were incubated in our *in vitro* C6/36 RNA deadenylation assay, and the relative rates of poly(A) tail shortening were analyzed. As seen in Fig. 4B, the SINV-RSE RNA showed a slow, distributive-like deadenylation pattern similar to that observed with the full 3' UTR. Interestingly, SINV-URE RNA, which contained only the U-rich region, also was substantially more stable than the reporter RNA. The presence of the SINV-CSE had no substantial effect on deadenylation efficiency. From these data, we conclude that both the RSE and U-rich segments of the 3' UTR play a major role in slowing the kinetics of deadenylation and likely contribute to the repression of deadenylation observed *in vivo*. Such a combinatorial arrange-

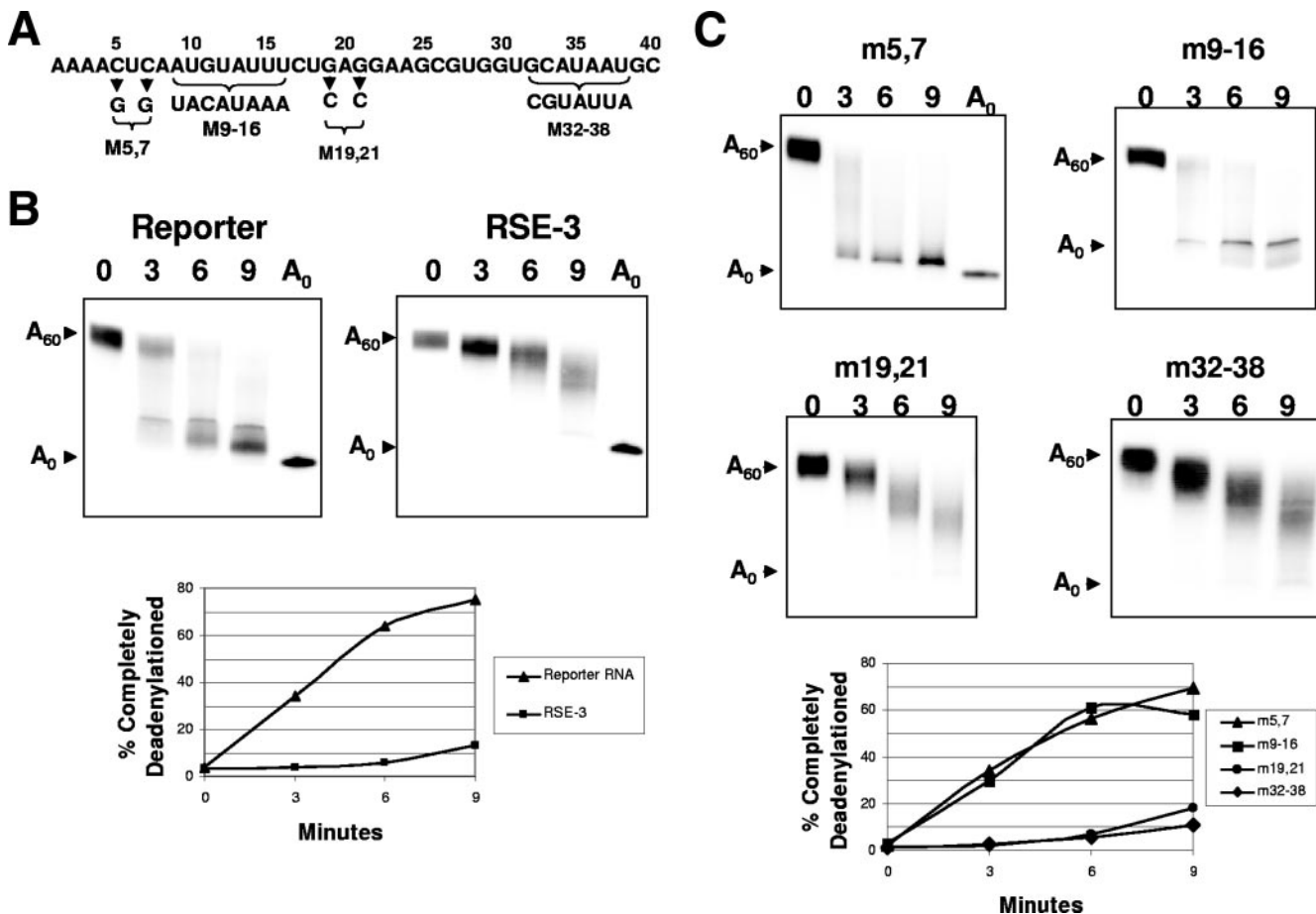


FIG. 5. An isolated SINV RSE can partially repress deadenylation. (A) The sequence of RSE3 from the SINV MRE16 strain. The base changes in the variants used in panel B are indicated below the sequence. (B) A polyadenylated reporter RNA (Reporter) or a variant containing RSE3 from SINV was incubated in an in vitro RNA deadenylation/decay system derived from C6/36 S100 cytoplasmic extracts for the indicated times. Reaction products were analyzed on a 5% polyacrylamide gel containing 7 M urea and visualized by phosphorimaging. The lanes marked A₀ contain fully deadenylated versions of the input transcript. The panel below is a graphical representation of the data. Similar data were obtained from multiple independent replicates. (C) Polyadenylated RNAs containing the mutations in the indicated bases of RSE3 were incubated in the in vitro RNA deadenylation/decay system as described above. The bottom panel is a graphical representation of the data. Similar results were obtained from multiple independent replicates.

ment of regulatory elements is not surprising, given the wide host range of the virus and considering that many regions of the 3' UTR act in concert to regulate the stability of cellular transcripts (50, 53).

The SINV RSE is a regulator of deadenylation efficiency. The evidence shown in Fig. 4 that a region containing the SINV RSEs blocks the apparent processivity of poly(A) tail shortening on viral RNA substrates represents a potential biological function for this conserved 3' UTR element. In order to further investigate a potential role for the SINV RSE in the repression of deadenylation, we isolated the nucleotide sequence comprising the third RSE (Fig. 5A), inserted it into the polyadenylated reporter RNA backbone, and assessed deadenylation patterns in our in vitro assay. As seen in Fig. 5B, this isolated single RSE significantly slowed deadenylation rates compared to the parent reporter RNA. To demonstrate that the repression of deadenylation rates observed was specific for the RSE sequence, we created a set of four constructs containing specific mutations within the RSE. As seen in Fig. 5C, while

RSE variants m19,21 and m32-38 were deadenylated in the slow, distributive pattern seen with the wild-type RSE3 RNA, both m5,7 and m9-16 RSE3 variants lost the ability to inhibit deadenylation. From these data we conclude that the SINV RSE influences the efficiency of deadenylation on RNAs and that sequences in the 5' half of the RSE appear to be necessary for the observed repression. While these data failed to implicate an RSE structure predicted by Mfold (Rensselaer Polytechnic Institute) in the regulation of deadenylation (data not shown), the potential contribution of secondary and higher-order RNA structures to the repression of deadenylation still remains to be fully determined.

The 3' UTR of SINV requires a *trans*-factor to inhibit deadenylation. Regulation of many posttranscriptional processes is often mediated by *trans*-acting proteins. Having explored the contribution of viral sequences in regulating deadenylation, we next wanted to determine if host proteins were contributing to this process through their interaction with the 3' UTR of SINV RNAs. To do this, we added a 50-fold molar excess of either

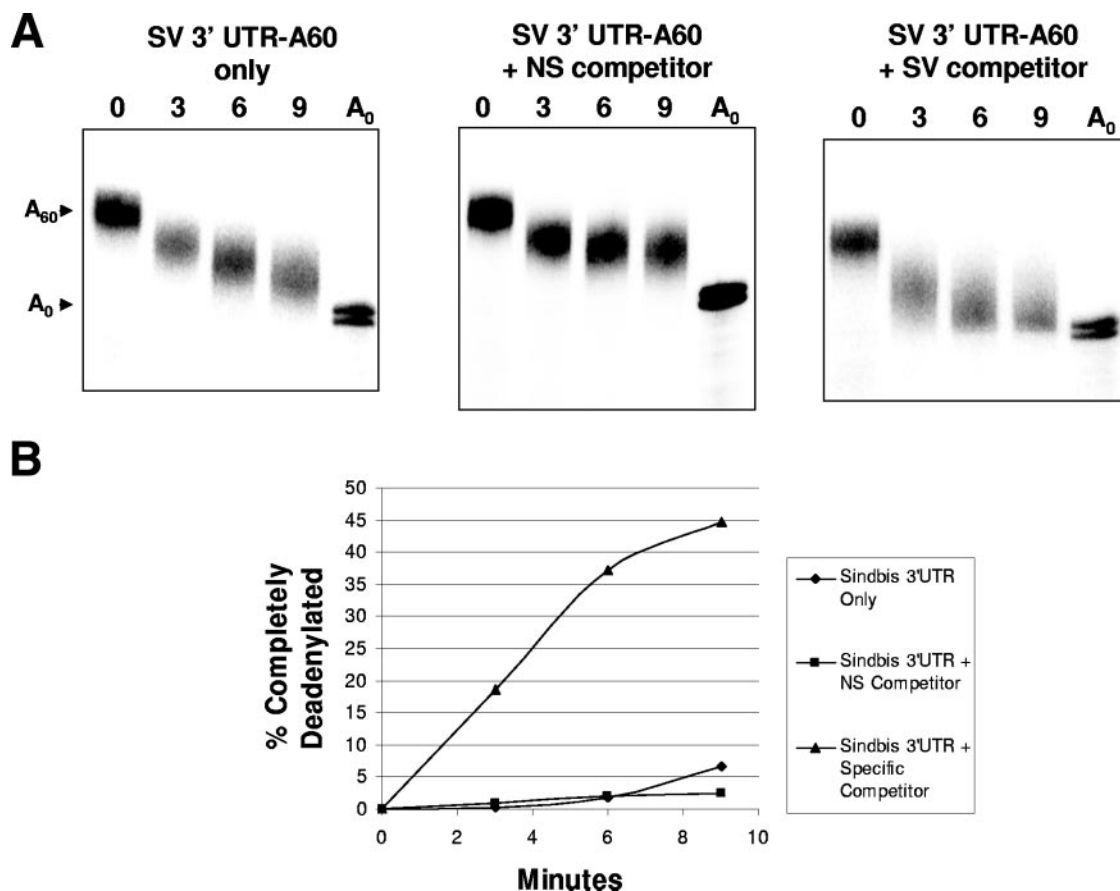


FIG. 6. A titratable *trans*-acting cellular factor contributes to the repression of deadenylation by the SINV 3' UTR. (A) Polyadenylated RNAs containing the SINV (SV) 3' UTR were incubated in the *in vitro* RNA deadenylation/decay system either in the absence of competitor RNA (left), the presence of a 50-fold molar excess of a nonspecific (NS) competitor RNA derived from pGem-4 polylinker sequences (middle), or a 50-fold molar excess of a specific competitor RNA derived from the SINV 3' UTR (right) for the indicated times. Reaction products were analyzed on a 5% polyacrylamide gel containing 7 M urea and visualized by phosphorimaging. The lanes marked A₀ contain fully deadenylated versions of the input transcript. (B) A graphical representation of the data from the experiments from panel A. Similar data were obtained from multiple independent replicates.

a nonspecific competitor RNA derived from the pGem4 polylinker sequence or a specific SINV 3' UTR-derived competitor RNA to our *in vitro* deadenylation assays. In this manner, we could assess the effect of each competitor on the deadenylation of a radiolabeled polyadenylated RNA containing the full 3' UTR of SINV. As seen in Fig. 6A and B, the addition of a nonspecific competitor did not substantially alter the slow, distributive-like deadenylation pattern of the SINV 3' UTR-A60 RNA. The addition of a SINV 3' UTR specific competitor, however, increased deadenylation efficiency over 10-fold. This SINV 3' UTR competitor RNA had no effect on the deadenylation efficiency of a reporter construct that lacked viral 3' UTR sequences (data not shown). These data clearly suggest that a titratable *trans*-factor(s) derived from the host cell is required for the SINV 3' UTR to effectively evade the cellular deadenylation apparatus.

In order to begin identifying candidate protein(s) contributing to the evasion of deadenylation by the viral 3' UTR in our C6/36 cell extracts, we used a competitor titration approach in conjunction with both functional deadenylation and UV cross-linking assays. This approach allowed us to associate the com-

petition of specific cross-linked proteins with activation of deadenylation by the competitor RNA. As seen in Fig. 7A, there was no effect on either the pattern of deadenylation (top panel) or the proteins that cross-linked to the SINV 3' UTR (bottom panel) in the presence of increasing amounts of a nonspecific, pGem4-derived competitor RNA. In contrast, when increasing amounts of a SINV 3' UTR-specific competitor RNA was added, deadenylation of the SINV 3' UTR-A60 RNA was partially activated by a 12.5- to 25-fold molar excess of competitor RNA and fully activated at a 50- to 100-fold excess (Fig. 7B, top panel). Interestingly, the competition of a 38-kDa cellular protein paralleled the level of specific competitor RNA required for activation of deadenylation of the SINV 3' UTR-A60 RNA (Fig. 7B, bottom panel). In addition, as the 38-kDa protein was competed from the radiolabeled RNA, a 32-kDa protein was observed to assemble on the 3' UTR. Neither competitor RNA affected the deadenylation efficiency or pattern of cross-linked proteins on a reporter RNA that lacked the SINV 3' UTR sequence (data not shown). Collectively, these data provide mechanistic insights into the repression of deadenylation by the SINV 3' UTR and suggest that

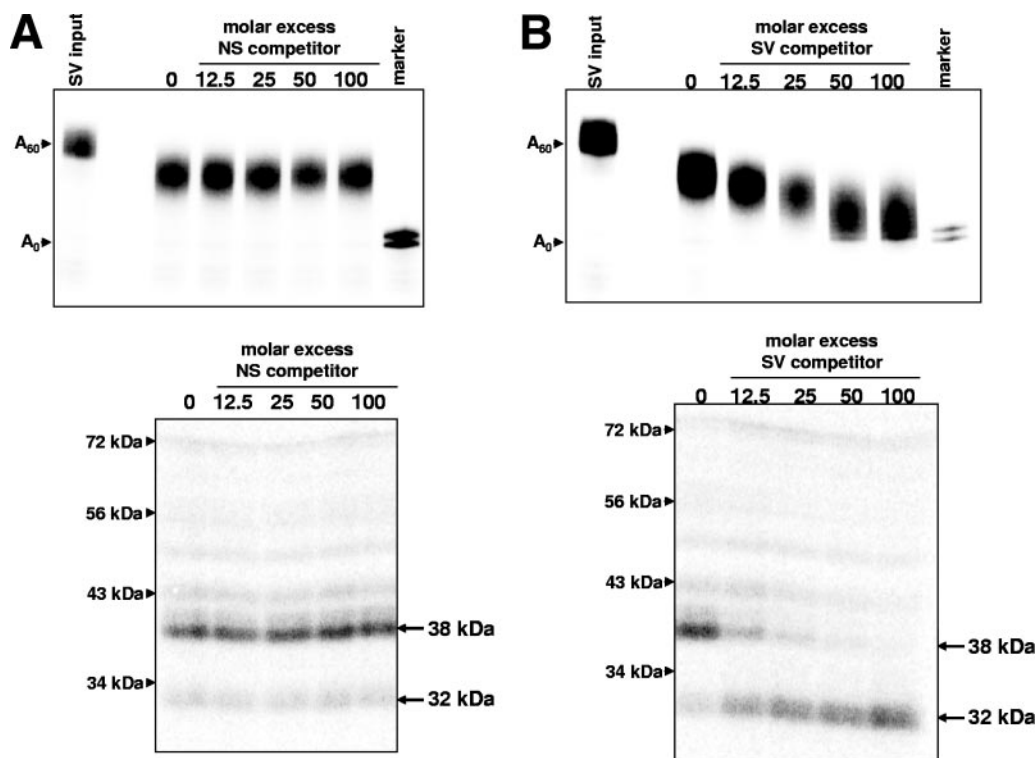


FIG. 7. The binding of a 38-kDa mosquito cell protein is strongly associated with the repression of deadenylation by the SINV 3' UTR. Polyadenylated RNAs containing the SINV 3' UTR were incubated in the *in vitro* RNA deadenylation/decay system for 9 min in the presence of the indicated amount of nonspecific (NS) competitor (Gem-A0) RNA (A) or a specific competitor (SV) derived from the SINV 3' UTR (B). The top panels of each section are the results of analysis of the RNA products of the reaction on denaturing 5% polyacrylamide gels. The SV input lanes indicate SINV-3' UTR-A60 transcripts that were not incubated in the *in vitro* system, and the marker lane indicates the position of a fully deadenylated version of the input transcript. The lower panels of each section are the results of UV cross-linking assays performed in parallel to the functional assays. Following incubation in the *in vitro* deadenylation/decay system, reaction mixtures were irradiated with UV light and treated with RNase, and proteins cross-linked to radioactive RNA oligomers were separated on 10% polyacrylamide gels containing SDS. The positions of size markers are indicated on the left of each gel, and the apparent molecular sizes of cross-linked proteins of interest are indicated on the right.

the binding of the cellular 38-kDa protein to the SINV 3' UTR is associated with a block of deadenylation whereas the interaction of the 32-kDa protein may function to promote deadenylation.

The 3' UTR of VEEV also represses deadenylation and competes with the 3' UTR of SINV for a common *trans*-acting factor. In order to generalize our observations to other members of the alphavirus family, we tested whether the 3' UTR of VEEV was also capable of protecting transcripts from deadenylation. Like SINV, the 3' UTR of VEEV contains a repeated RSE element. However, the RSEs of VEEV contain little sequence similarity to the SINV RSE (51). As seen in Fig. 8A, the addition of the 3' UTR of VEEV into the Gem-4 reporter construct resulted in an effective block to deadenylation activity in our *in vitro* system, similar to that observed for the SINV 3' UTR. Furthermore, competition analyses demonstrated that a *trans*-acting factor was involved in mediating the repression of deadenylation by the VEEV 3' UTR. As seen in Fig. 8B, while the addition of a nonspecific competitor RNA had no effect on deadenylation of a VEEV 3' UTR-A60 RNA, the addition of the VEEV 3' UTR as a competitor resulted in very effective poly(A) shortening of the RNA substrate in extracts. UV cross-linking analysis demonstrated that a 38-kDa protein was specifically associated with the VEEV 3' UTR

(Fig. 8C, left panel). Thus, it is likely that the same 38-kDa protein that interacts with the SINV 3' UTR is associated with deadenylation repression (Fig. 7). Interestingly, the addition of VEEV competitor RNA effectively competes for this 38-kDa protein with a radiolabeled SINV 3' UTR substrate (Fig. 8C, right panel), further suggesting a mechanistic similarity between SINV and VEEV repression of deadenylation. Therefore, we conclude that the ability to repress deadenylation by the 3' UTR is conserved in a distinct member of the alphavirus family. In addition, binding and cross-competition analysis provide further evidence suggesting that a 38-kDa protein may play an important role in mediating the repression of deadenylation by alphavirus 3' UTRs.

DISCUSSION

This study outlines five key points that argue for a role for cellular mRNA decay enzymes in the SINV life cycle. First, SINV RNAs are clearly degraded with a measurable half-life during the course of an infection. Therefore, viral RNAs must interface with the cellular mRNA decay machinery during an infection. Second, the viral RNAs are refractory, particularly in cells, to deadenylation—the initial event in the major pathway of mRNA decay in the cell. This suggests that SINV has

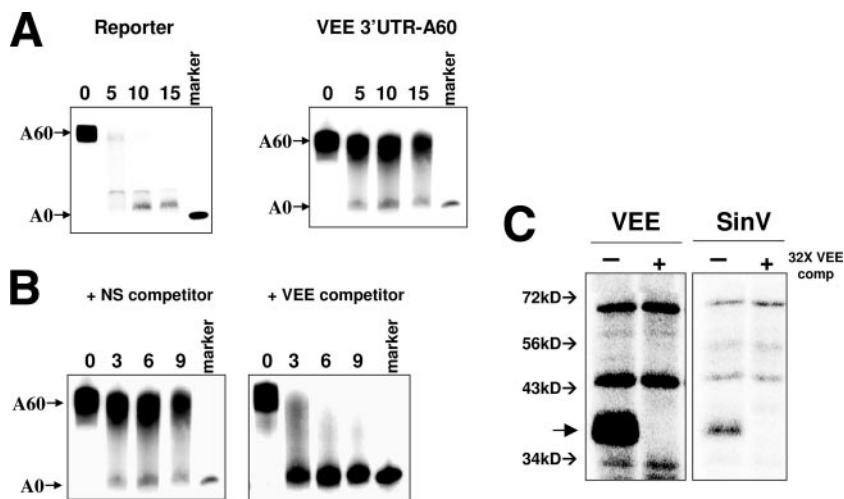


FIG. 8. The 3' UTR of VEEV also represses deadenylation and interacts with a 38-kDa protein. (A) The Gem-4 reporter RNA or a derivative that contains the 3' UTR of VEEV was incubated in the *in vitro* C6/36 deadenylation system for the times indicated. Reaction products were analyzed on a 5% polyacrylamide gel containing 7 M urea and visualized by phosphorimaging. The marker lanes contain fully deadenylated versions of the input transcript. (B) Polyadenylated VEEV 3' UTR-A60 RNA was incubated in the *in vitro* deadenylation system derived from C6/36 S100 cytoplasmic extracts in the presence of a 32-fold molar excess of either a nonspecific competitor (+NS) derived from pGem-4 or a specific competitor RNA containing VEEV 3' UTR sequences (+VEE). Reaction products were analyzed on a 5% polyacrylamide gel containing 7 M urea and visualized by phosphorimaging. The marker lanes contain fully deadenylated versions of the input transcript. (C) Radiolabeled VEEV 3' UTR-A60 RNA or SINV 3' UTR-A60 RNA was incubated with C6/36 S100 cytoplasmic extracts in the *in vitro* deadenylation system in the absence (–) or presence (+) of a 32-fold molar excess of an unlabeled VEEV 3' UTR competitor RNA. Reaction mixtures were irradiated with UV light and treated with RNase, and proteins cross-linked to radioactive RNA oligomers were separated on 10% polyacrylamide gels containing SDS. The positions of size markers are indicated on the left.

evolved a strategy to evade the major cellular decay enzymes, an adaptation that may significantly contribute to a productive infection. Third, a conserved feature of the alphavirus 3' UTR, the RSEs, is part of a combinatorial set of regions in the 3' UTR that mediates the repression of deadenylation. The conservation of this feature suggests that the ability to repress deadenylation could be a common feature of alphaviral 3' UTRs. Fourth, the interaction between the viral 3' UTR and a 38-kDa cellular protein is strongly associated with the observed block in deadenylation, suggesting a possible mechanism for the repression of poly(A) shortening which involves the usurping of cellular factors. Finally, the 3' UTR from VEEV also represses deadenylation and interacts with a 38-kDa cellular protein, suggesting that a common strategy for inhibiting poly(A) tail shortening may be conserved among alphaviruses. Collectively, these data suggest that the influence of cellular mRNA decay enzymes must be taken into account if one is to fully appreciate the molecular biology of SINV, and likely other, viral infections.

Why would it be important for SINV to actively stabilize its transcripts, particularly the subgenomic mRNA that is so actively transcribed? The answer to this question likely involves the fact that levels of mRNAs are determined by both transcription and degradation rates. The fact that the subgenomic RNA is being transcribed throughout the infection is not sufficient to ensure its accumulation to physiological levels in the cell. Many cellular mRNAs are actively transcribed in the cell but accumulate only under specific conditions due to the fact that they are very actively degraded in a regulated manner (22). Therefore, effective accumulation of viral transcripts requires that they possess a means to avoid rapid degradation by

the cellular mRNA decay machinery. In addition, maintenance of a poly(A) tail is also necessary to ensure efficient translation of viral mRNAs.

Our ability to readily assess SINV mRNA decay revolved around two technologies, the use of a temperature-sensitive viral polymerase variant *in vivo* and the application of a cell-free *in vitro* system. Both of these experimental approaches are likely readily applicable to other viruses. Temperature-sensitive RNA polymerases have been described for numerous viruses (see, e.g., references 15 and 16) and should be relatively easy to incorporate into recombinant constructs. This strategy allows one to specifically turn off viral RNA synthesis to allow the assessment of decay without any confounding secondary effects of drugs (26, 36). Our *in vitro* mRNA system from C6/36 cells (42, 49) is an adaptation of technology that we have previously developed and extensively exploited in HeLa cells (19) and other eukaryotic systems (39, 56) to gain mechanistic insights into mRNA decay. Application of a combination of these approaches should provide a powerful tool to analyze the contribution of mRNA decay to viral infections.

In vivo and *in vitro* data clearly indicate that SINV RNAs have developed a means to maintain the integrity of their poly(A) tails and avoid deadenylation. This is particularly interesting because most mRNA decay initiates via this pathway (22). In addition, transfected RNAs (which also are largely, if not exclusively, cytoplasmic) are also actively deadenylated (47), further emphasizing the unique stability of SINV mRNAs. Despite being refractory to deadenylation, SINV RNAs are still clearly degraded (Fig. 1). This implies the involvement of an alternative, deadenylation-independent pathway. There are several pathways of RNA decay in the cell that

do not necessarily initiate with poly(A) tail shortening, including nonsense-mediated decay (1, 3), RNA interference (46), and endonucleolytic decay (61). An interesting question for future work will be to assess whether any of these known deadenylation-independent pathways, or perhaps a novel pathway, is responsible for the observed decay of viral mRNAs. Once the pathway(s) is identified, it may be possible to stimulate this pathway(s) of viral mRNA decay, creating a hostile environment for viral growth while having perhaps minimal effects on cellular gene expression.

Numerous deadenylase enzymes have been described in eukaryotic cells (22), with CCR4, PAN2/3, and PARN among the major, most studied activities. One important question is whether the SINV 3' UTR is capable of repressing the action of all deadenylases on viral transcripts or if it targets only specific enzymes. Since the 5' cap-stimulated PARN enzyme (12, 20, 37) appears to be the major deadenylase in C6/36 mosquito cell extracts (42), our *in vitro* data would suggest that this enzyme is at least one target of the repressive effect of the 3' UTR. Future studies using a combination of RNA interference knock-downs and *in vitro* reconstitution analyses will be required to assess the influence of the SINV 3' UTR on the enzymatic activity of other deadenylases.

The results of our deletion analyses (Fig. 4) suggest that multiple regions of the 3' UTR influence the stability of SINV mRNAs. The mapping of a deadenylation repression element to RSE sequences provides the first biological function for this conserved feature of alphavirus 3' UTRs. The core element may be repeated in its natural context in order to amplify repression through the additive effects of individual copies as has been seen in tethering experiments (2). Combinatorial arrangements of mRNA stability elements have also been identified in cellular mRNAs (50, 53), suggesting that such an organization may be relatively common for regulated mRNAs. It will be interesting to see if the apparently unrelated RSEs of other alphaviruses such as VEEV possess a similar ability to repress deadenylation. The combination of multiple mRNA stabilizers in SINV may also contribute to the broad host range of the virus, as well as the relative overall effectiveness of a viral infection. In this regard, it is interesting that deletions of the 3' UTR that remove the deadenylation-repression region described here were shown by Kuhn et al. to result in a defective virus that grows very poorly in mosquito C6/36 cells (33). Defects in the ability of the 3' UTR mutant virus to repress deadenylation could be at least partially responsible for these growth defects.

As shown in Fig. 7 and 8, the interaction of a 38-kDa protein with the SINV and VEEV 3' UTRs is strongly associated with a repression of deadenylation. The ability to combine protein binding/competition studies with functional assays as shown here demonstrates one of the advantages of the *in vitro* system used in these studies. Given its relative molecular size, this 38-kDa protein could be the *Aedes* homolog of any number of a known cellular RNA stabilizers, including HuR (9), TIA-1/TIAR (17), or numerous others. Alternatively, the 38-kDa protein could also be a novel cellular protein that the virus has specifically usurped to remodel the messenger ribonucleoprotein composition of its 3' UTR. It is important to point out that the UV cross-linking approach used in this study does not involve any purification steps. Identification of the 38-kDa

protein, therefore, will require the application of affinity-based or conventional chromatographic methods.

In summary, the cellular mRNA decay machinery plays a very major role in host cell gene expression and quality control. The underlying hypothesis of this work is that viruses very likely have had to evolve a way to adapt to, and perhaps usurp, this powerful machinery. SINV and VEEV RNAs, through their 3' UTRs, have evolved a novel way to avoid a major mRNA decay pathway in the cell and ensure efficient translation by maintenance of their poly(A) tails. Future questions include the identification of the mechanistic basis of the repression of deadenylation, the conservation of the ability to repress deadenylation among other alphaviruses, and the characterization of the apparently unusual, deadenylation-independent pathway of mRNA decay that acts upon these viral transcripts. Answers to these questions will allow the full impact of the cellular mRNA stability system on viral gene expression and growth to be assessed.

ACKNOWLEDGMENTS

We thank Irma Sanchez-Vargas, Carol Blair, Richard Kinney, and Ken Olson for reagents and invaluable advice; Erica Suchman, Jon Carlson, and Joe Piper for C6/36 spinner cells; Margaret MacDonald for her generous gift of pToto1101/ts6; Justin Curnutt for construction of the VEEV 3' UTR plasmids; and members of the Wilusz laboratory for helpful discussions.

N.L.G. was supported by USDA Cooperative State Research, Education, and Extension Service training grant 2005-38420-15813. This work was supported by NIH grant AI063434 to J.W.

REFERENCES

- Amrani, N., M. S. Sachs, and A. Jacobson. 2006. Early nonsense: mRNA decay solves a translational problem. *Nat. Rev. Mol. Cell Biol.* 7:415–425.
- Baron-Benhamou, J., N. H. Gehring, A. E. Kulozik, and M. W. Hentze. 2004. Using the λ N peptide to tether proteins to RNAs. *Methods Mol. Biol.* 257:135–154.
- Behm-Ansmant, I., and E. Izaurralde. 2006. Quality control of gene expression: a stepwise assembly pathway for the surveillance complex that triggers nonsense-mediated mRNA decay. *Genes Dev.* 20:391–398.
- Bick, M. J., J. W. Carroll, G. Gao, S. P. Goff, C. M. Rice, and M. R. MacDonald. 2003. Expression of the zinc-finger antiviral protein inhibits alphavirus replication. *J. Virol.* 77:11555–11562.
- Chang, Y. F., J. S. Imam, and M. F. Wilkinson. 2007. The nonsense-mediated decay RNA surveillance pathway. *Annu. Rev. Biochem.* 76:51–74.
- Cheadle, C., J. Fan, Y. S. Cho-Chung, T. Werner, J. Ray, L. Do, M. Gorospe, and K. G. Becker. 2005. Control of gene expression during T cell activation: alternate regulation of mRNA transcription and mRNA stability. *BMC Genomics* 6:75.
- Cheadle, C., J. Fan, Y. S. Cho-Chung, T. Werner, J. Ray, L. Do, M. Gorospe, and K. G. Becker. 2005. Stability regulation of mRNA and the control of gene expression. *Ann. N. Y. Acad. Sci.* 1058:196–204.
- Chen, C. Y., and A. B. Shyu. 2003. Rapid deadenylation triggered by a nonsense codon precedes decay of the RNA body in a mammalian cytoplasmic nonsense-mediated decay pathway. *Mol. Cell. Biol.* 23:4805–4813.
- Cherry, J., V. Karschner, H. Jones, and P. H. Pekala. 2006. HuR, an RNA-binding protein, involved in the control of cellular differentiation. *In Vivo* 20:17–23.
- Conrad, N. K., S. Mili, E. L. Marshall, M. D. Shu, and J. A. Steitz. 2006. Identification of a rapid mammalian deadenylation-dependent decay pathway and its inhibition by a viral RNA element. *Mol. Cell* 24:943–953.
- Decker, C. J., and R. Parker. 1993. A turnover pathway for both stable and unstable mRNAs in yeast: evidence for a requirement for deadenylation. *Genes Dev.* 7:1632–1643.
- Dehlin, E., M. Wormington, C. G. Korner, and E. Wahle. 2000. Cap-dependent deadenylation of mRNA. *EMBO J.* 19:1079–1086.
- Eulalio, A., I. Behm-Ansmant, and E. Izaurralde. 2007. P bodies: at the crossroads of post-transcriptional pathways. *Nat. Rev. Mol. Cell Biol.* 8:9–22.
- Eulalio, A., I. Behm-Ansmant, D. Schweizer, and E. Izaurralde. 2007. P-body formation is a consequence, not the cause, of RNA-mediated gene silencing. *Mol. Cell. Biol.* 27:3970–3981.
- Feller, J. A., S. Smallwood, M. H. Skiadopoulos, B. R. Murphy, and S. A. Moyer. 2000. Comparison of identical temperature-sensitive mutations in the

- L polymerase proteins of Sendai and parainfluenza 3 viruses. *Virology* **276**:190–201.
16. Fodor, E., M. Crow, L. J. Mingay, T. Deng, J. Sharps, P. Fechter, and G. G. Brownlee. 2002. A single amino acid mutation in the PA subunit of the influenza virus RNA polymerase inhibits endonucleolytic cleavage of capped RNAs. *J. Virol.* **76**:8989–9001.
 17. Forch, P., and J. Valcarcel. 2001. Molecular mechanisms of gene expression regulation by the apoptosis-promoting protein TIA-1. *Apoptosis* **6**:463–468.
 18. Ford, L. P., and J. Wilusz. 1999. 3'-Terminal RNA structures and poly(U) tracts inhibit initiation by a 3'→5' exonuclease in vitro. *Nucleic Acids Res.* **27**:1159–1167.
 19. Ford, L. P., and J. Wilusz. 1999. An in vitro system using HeLa cytoplasmic extracts that reproduces regulated mRNA stability. *Methods* **17**:21–27.
 20. Gao, M., D. T. Fritz, L. P. Ford, and J. Wilusz. 2000. Interaction between a poly(A)-specific ribonuclease and the 5' cap influences mRNA deadenylation rates in vitro. *Mol. Cell* **5**:479–488.
 21. Garcia-Martinez, J., A. Aranda, and J. E. Perez-Ortin. 2004. Genomic run-on evaluates transcription rates for all yeast genes and identifies gene regulatory mechanisms. *Mol. Cell* **15**:303–313.
 22. Garneau, N. L., J. Wilusz, and C. J. Wilusz. 2007. The highways and byways of mRNA decay. *Nat. Rev. Mol. Cell Biol.* **8**:113–126.
 23. Greenberg, M. E., A. B. Shyu, and J. G. Belasco. 1990. Deadenylation: a mechanism controlling c-fos mRNA decay. *Enzyme* **44**:181–192.
 24. Hardy, R. W., and C. M. Rice. 2005. Requirements at the 3' end of the Sindbis virus genome for efficient synthesis of minus-strand RNA. *J. Virol.* **79**:4630–4639.
 25. Harris, D., Z. Zhang, B. Chaubey, and V. N. Pandey. 2006. Identification of cellular factors associated with the 3'-nontranslated region of the hepatitis C virus genome. *Mol. Cell. Proteomics* **5**:1006–1018.
 26. Harrold, S., C. Genovese, B. Kobrin, S. L. Morrison, and C. Milcarek. 1991. A comparison of apparent mRNA half-life using kinetic labeling techniques vs decay following administration of transcriptional inhibitors. *Anal. Biochem.* **198**:19–29.
 27. Houseley, J., J. LaCava, and D. Tollervey. 2006. RNA-quality control by the exosome. *Nat. Rev. Mol. Cell Biol.* **7**:529–539.
 28. Hughes, T. A. 2006. Regulation of gene expression by alternative untranslated regions. *Trends Genet.* **22**:119–122.
 29. Jacobson, A., and S. W. Peltz. 1996. Interrelationships of the pathways of mRNA decay and translation in eukaryotic cells. *Annu. Rev. Biochem.* **65**:693–739.
 30. Karpf, A. R., J. M. Blake, and D. T. Brown. 1997. Characterization of the infection of *Aedes albopictus* cell clones by Sindbis virus. *Virus Res.* **50**:1–13.
 31. Kim, J. H., and J. D. Richter. 2006. Opposing polymerase-deadenylase activities regulate cytoplasmic polyadenylation. *Mol. Cell* **24**:173–183.
 32. Kren, B. T., and C. J. Steer. 1996. Posttranscriptional regulation of gene expression in liver regeneration: role of mRNA stability. *FASEB J.* **10**:559–573.
 33. Kuhn, R. J., Z. Hong, and J. H. Strauss. 1990. Mutagenesis of the 3' nontranslated region of Sindbis virus RNA. *J. Virol.* **64**:1465–1476.
 34. Laird-Offringa, I. A., C. L. de Wit, P. Elfferich, and A. J. van der Eb. 1990. Poly(A) tail shortening is the translation-dependent step in c-myc mRNA degradation. *Mol. Cell. Biol.* **10**:6132–6140.
 35. Levis, R., B. G. Weiss, M. Tsiang, H. Huang, and S. Schlesinger. 1986. Deletion mapping of Sindbis virus DI RNAs derived from cDNAs defines the sequences essential for replication and packaging. *Cell* **44**:137–145.
 36. Loreni, F., G. Thomas, and F. Amaldi. 2000. Transcription inhibitors stimulate translation of 5' TOP mRNAs through activation of S6 kinase and the mTOR/FRAP signalling pathway. *Eur. J. Biochem.* **267**:6594–6601.
 37. Martinez, J., Y. G. Ren, P. Nilsson, M. Ehrenberg, and A. Virtanen. 2001. The mRNA cap structure stimulates rate of poly(A) removal and amplifies processivity of degradation. *J. Biol. Chem.* **276**:27923–27929.
 38. Meyer, S., C. Temme, and E. Wahle. 2004. Messenger RNA turnover in eukaryotes: pathways and enzymes. *Crit. Rev. Biochem. Mol. Biol.* **39**:197–216.
 39. Milone, J., J. Wilusz, and V. Bellofatto. 2004. Characterization of deadenylation in trypanosome extracts and its inhibition by poly(A)-binding protein Pab1p. *RNA* **10**:448–457.
 40. Muhrad, D., C. J. Decker, and R. Parker. 1994. Deadenylation of the unstable mRNA encoded by the yeast MFA2 gene leads to decapping followed by 5'→3' digestion of the transcript. *Genes Dev.* **8**:855–866.
 41. Murray, E. L., and D. R. Schoenberg. 2007. A+U-rich instability elements differentially activate 5'-3' and 3'-5' mRNA decay. *Mol. Cell. Biol.* **27**:2791–2799.
 42. Opyrchal, M., J. R. Anderson, K. J. Sokolowski, C. J. Wilusz, and J. Wilusz. 2005. A cell-free mRNA stability assay reveals conservation of the enzymes and mechanisms of mRNA decay between mosquito and mammalian cell lines. *Insect Biochem. Mol. Biol.* **35**:1321–1334.
 43. Osborne, H. B., Gautier-Court, A. Graindorge, C. Barreau, Y. Audic, R. Thuret, N. Pollet, and L. Paillard. 2005. Post-transcriptional regulation in *Xenopus* embryos: role and targets of EDEN-BP. *Biochem. Soc. Trans.* **33**:1541–1543.
 44. Peng, Y., and D. R. Schoenberg. 2007. c-Src activates endonuclease-mediated mRNA decay. *Mol. Cell* **25**:779–787.
 45. Pogue, G. P., C. C. Huntley, and T. C. Hall. 1994. Common replication strategies emerging from the study of diverse groups of positive-strand RNA viruses. *Arch. Virol. Suppl.* **9**:181–194.
 46. Rana, T. M. 2007. Illuminating the silence: understanding the structure and function of small RNAs. *Nat. Rev. Mol. Cell Biol.* **8**:23–36.
 47. Seal, R., R. Temperley, J. Wilusz, R. N. Lightowlers, and Z. M. Chrzanoska-Lightowlers. 2005. Serum-deprivation stimulates cap-binding by PARN at the expense of eIF4E, consistent with the observed decrease in mRNA stability. *Nucleic Acids Res.* **33**:376–387.
 48. Simon, E., S. Camier, and B. Seraphin. 2006. New insights into the control of mRNA decapping. *Trends Biochem. Sci.* **31**:241–243.
 49. Sokolowski, K., J. R. Anderson, and J. Wilusz. 2007. Development of an in vitro mRNA decay system in insect cells, p. 277–288. *In* J. Wilusz (ed.), *Post-transcriptional control of gene expression*. Humana Press, Totowa, NJ.
 50. Stocklin, G., M. Lu, B. Rattenbacher, and C. Moroni. 2003. A constitutive decay element promotes tumor necrosis factor alpha mRNA degradation via an AU-rich element-independent pathway. *Mol. Cell. Biol.* **23**:3506–3515.
 51. Strauss, J. H., and E. G. Strauss. 1994. The alphaviruses: gene expression, replication, and evolution. *Microbiol. Rev.* **58**:491–562.
 52. Suchman, E., and J. Carlson. 2004. Production of mosquito denonucleosis viruses by *Aedes albopictus* C6/36 cells adapted to suspension culture in serum-free protein-free media. *In Vitro Cell. Dev. Biol. Anim.* **40**:74–75.
 53. Sureban, S. M., N. Murmu, P. Rodriguez, R. May, R. Maheshwari, B. K. Dieckgraefe, C. W. Houchen, and S. Anant. 2007. Functional antagonism between RNA binding proteins HuR and CUGBP2 determines the fate of COX-2 mRNA translation. *Gastroenterology* **132**:1055–1065.
 54. Tucker, M., R. R. Staples, M. A. Valencia-Sanchez, D. Muhrad, and R. Parker. 2002. Ccr4p is the catalytic subunit of a Ccr4p/Pop2p/Notp mRNA deadenylase complex in *Saccharomyces cerevisiae*. *EMBO J.* **21**:1427–1436.
 55. Wilson, T., and R. Treisman. 1994. Removal of poly(A) and consequent degradation of c-fos mRNA facilitated by 3' AU-rich sequences. *Nature* **336**:396–399.
 56. Wilusz, C. J., M. Gao, C. L. Jones, J. Wilusz, and S. W. Peltz. 2001. Poly(A)-binding proteins regulate both mRNA deadenylation and decapping in yeast cytoplasmic extracts. *RNA* **7**:1416–1424.
 57. Wilusz, J., and T. Shenk. 1988. A 64 kd nuclear protein binds to RNA segments that include the AAUAAA polyadenylation motif. *Cell* **52**:221–228.
 58. Xu, N., C. Y. Chen, and A. B. Shyu. 1997. Modulation of the fate of cytoplasmic mRNA by AU-rich elements: key sequence features controlling mRNA deadenylation and decay. *Mol. Cell. Biol.* **17**:4611–4621.
 59. Xu, N., P. Loffin, C. Y. Chen, and A. B. Shyu. 1998. A broader role for AU-rich element-mediated mRNA turnover revealed by a new transcriptional pulse strategy. *Nucleic Acids Res.* **26**:558–565.
 60. Yamashita, A., T. C. Chang, Y. Yamashita, W. Zhu, Z. Zhong, C. Y. Chen, and A. B. Shyu. 2005. Concerted action of poly(A) nucleases and decapping enzyme in mammalian mRNA turnover. *Nat. Struct. Mol. Biol.* **12**:1054–1063.
 61. Yang, F., Y. Peng, E. L. Murray, Y. Otsuka, N. Kedersha, and D. R. Schoenberg. 2006. Polysome-bound endonuclease PMR1 is targeted to stress granules via stress-specific binding to TIA-1. *Mol. Cell. Biol.* **26**:8803–8813.
 62. Zangar, R. C., M. Hernandez, T. A. Kocarek, and R. F. Novak. 1995. Determination of the poly(A) tail lengths of a single mRNA species in total hepatic RNA. *BioTechniques* **18**:465–469.